Mo-Doped La_2O_3 as Charge-Trapping Layer for Improved Low-Voltage Flash-Memory Performance

Q. B. Tao, P. T. Lai*

Department of Electrical & Electronic Engineering, the University of Hong Kong, Pokfulam Road, Hong Kong

E-mail: laip@eee.hku.hk

Abstract

To utilize the negative conduction-band offset of high-*K* MoO_3 with respect to Si, the memory characteristics of high-*K* La_2O_3 with and without Mo doping as charge-trapping layer were investigated. The cross-sectional structure of the memory was studied by transmission electron microscopy, and the chemical composition of the charge-trapping layer was investigated by X-ray photoelectron spectroscopy. Compared to the memory with pure La_2O_3, the one with Mo-doped La_2O_3 had a significantly large C-V hysteresis window, much higher programming/erasing speeds and better charge retention because the Mo doping introduced many deeper-level traps and the LaMoO charge-trapping layer provided deeper quantum wells.

Introduction

Metal-oxide-nitride-oxide-silicon (MONOS)-type memories have attracted significant interest due to their lower operating voltage, higher program/erase (P/E) speeds, higher reliability and stronger scaling ability.[1-3] Many high-*K* dielectrics, especially rare-earth metal oxide materials, e.g. Pr_2O_3 (~15),[4] Nd_2O_3 (~16),[4] Er_2O_3 (~13),[4] and La_2O_3 (~27),[5] have been investigated as charge-trapping layer (CTL) due to their moderately high dielectric constant, wide bandgap and good electrical properties.[6] Among these dielectric materials, La_2O_3 is a promising one due to its large dielectric constant, thermodynamic compatibility with Si, and deep-level traps.[7] However, it has been reported that MONOS memory with La_2O_3 as CTL possesses a relatively small window due to its low trap density.[5] Recently, MoO_x has been proposed as the charge trapping site for nanocrystal memory and resulted in good memory performances, such as low operating voltage and good charge retention.[8, 9] However, for practical applications, uniform deposition or self-assembly of small nanocrystals is a necessary condition.[10-14] On the other hand, the application of MoO_3 for MONOS-type memory was seldom studied, even though MoO_3 has large dielectric constant (30~40),[15] many oxygen deficiencies as charge traps,[16] and large negative conduction-band offset (NCBO) with respect to Si.[17] Thus, in order to combine the advantages of both La_2O_3 and MoO_3, in this work, we propose Mo-doped La_2O_3 as a new CTL and study its memory characteristics for potential flash memory applications.

Experiment

MONOS capacitors were fabricated on p-type silicon wafers with a resistivity of 5 ~ 10 Ω•cm. Prior to the thermal growth of tunnel layer (SiO_2) in dry oxygen at 900 ^{0}C,

the Si wafers were cleaned by the standard RCA method. Then, sputtering was employed for the growth of CTL. La_2O_3 CTL (denoted as LaO sample) was deposited by sputtering of La metal target (RF = 30 W) in an Ar/O_2 (24:3) mixture at 2.1 mTorr for 4,200 s, while LaMoO CTL (denoted as LaMO sample) was deposited by co-sputtering of La metal target (RF = 30 W) and Mo metal target (DC = 0.01 A) in the same ambient for 2,700 s. After that, Al_2O_3 film as blocking layer was grown by means of atomic layer deposition. Subsequently, both samples went through post-deposition annealing at 900 ^{0}C in N_2 for 30 s. Following that, Al was thermally evaporated and patterned as gate electrode. Finally, the samples after Al evaporation on the wafer backside went through a forming-gas annealing at 300 ^{0}C for 20 min. The chemical composition of the CTLs in the MONOS capacitors was analyzed by X-ray photoelectron spectroscopy (XPS), while the physical thicknesses of the layers in the MONOS capacitor structure were confirmed by transmission electron microscopy (TEM).

Results and discussion

The structure of the MONOS capacitor is displayed in Fig. 1 (a). From the cross-sectional TEM image, it is observed that the physical thickness of the tunnel layer (SiO_2), the charge-trapping layer (LaMoO) and the blocking layer (Al_2O_3) is 4.2 nm, 6.5 nm and 14.5 nm respectively. The TEM image also verifies that the LaMoO film maintains amorphous structure after the PDA at 900 ^{0}C, and thus is suitable to be a CTL. To fairly compare the electrical performance of the two samples, the physical thickness of La_2O_3 (6.1 nm) is similar to that of LaMoO. The chemical binding states of both CTLs are investigated by XPS. Fig. 1 (b) shows the La 3*d* XPS spectrum of the La_2O_3 film and the LaMoO film. For the La_2O_3 film, there are two peaks of La 3*d* located at 834.2 eV and 850.9 eV, each possessing a satellite peak due to charge transfer between the metal atom and its oxygen ligand.[18] For the LaMoO film, both peaks of La 3*d* shift by 0.5 eV to higher values at 834.7 eV and 851.4 eV, which are consistent with the La component in binary metal oxide.[18] The possible reason for this shift is the oxygen reduction in the bulk of the LaMoO film due to the Mo incorporation. However, more studies are required to further investigate this phenomenon. Fig. 1 (c) also depicts the Mo 3*d* core level spectra of the LaMoO film. After fitting, two doublets are observed, one located at a higher binding energy of 235.6 eV (Mo $3d_{3/2}$) and 232.4 eV (Mo $3d_{5/2}$), while the other located at a lower binding energy of 234.9 eV (Mo $3d_{3/2}$) and 231.7 eV (Mo $3d_{5/2}$). It has been demonstrated that these peaks should result from the chemical states of Mo^{6+} and Mo^{5+} respectively,[16] and electrons can be trapped at Mo^{5+} sites in the vicinity of oxygen vacancies.[15] As explained above, these oxygen vacancies also reduce the oxygen content in the bulk of the LaMoO film, thus possibly resulting in a shift of the La 3*d* binding energy to higher values.

Fig. 2 shows the C-V hysteresis of the LaO sample and LaMO sample. The LaO sample has a smaller hysteresis window of 1.8 V under a +/-8 V sweep voltage. However, for the LaMO sample, the hysteresis window reaches 3.1 V even under a lower sweep voltage of +/-6 V, and further increases to 5.6 V and 7.1 V under +/-8 V and +/-10 V sweep respectively. The significantly larger C-V hysteresis window (about 3 times for the +/-8 V sweep) of the LaMO sample means that the Mo doping introduces many new traps in its CTL. Moreover, the *K* value of La_2O_3 film and LaMoO film can be calculated to be 12.8 and 16.5 respectively, by assuming a dielectric constant of 9 for the Al_2O_3 blocking layer. In addition, the Mo incorporation hardly affects the gate leakage current, which is 4.0×10^{-7} A/cm^2 and 3.8×10^{-7}

A/cm^2 at 10 V for the LaO and LaMO samples respectively. At 14 V, the same gate leakage current is 6.5×10^{-7} A/cm^2 and 1.2×10^{-6} A/cm^2 respectively.

The transient program and erase characteristics of the two samples are depicted in Fig. 3 (a) and (b) respectively. As can be seen, the LaMO sample has much higher programming speed than the LaO sample at the same applied voltage for the same pulse time. For the LaO sample at a program voltage of +14 V for a pulse time of 10 ms, 100 ms and 1 s, the V_{fb} shift is only 2.78 V, 3.54 V and 3.98 V respectively, while the corresponding shift of the LaMO sample is much larger: 5.87 V, 6.18 V and 6.50 V. Even at a lower program voltage of +10 V, the LaMO sample can still produce a larger shift of 3.88 V, 4.26 V and 4.50 V. This observation is consistent with the distinct C-V hysteresis difference of the two samples shown in Fig. 2. The faster programming characteristic of the LaMO sample should result from (i) the higher trap density in its CTL induced by the Mo doping because the Mo^{5+} sites in the vicinity of oxygen vacancies can act as charge traps (as explained earlier); (ii) the deeper quantum wells built by the energy-band alignment of the LaMoO CTL to the SiO_2 tunnel layer and Al_2O_3 blocking layer because the LaMoO film has a lower conduction band than the pure La_2O_3 film; (iii) the higher electric field in the SiO_2 tunnel layer because the Mo-doped La_2O_3 film has a higher dielectric constant than the pure La_2O_3 film. Fig. 3 (b) also shows that the LaMO sample has higher erasing speeds. Owing to the negative conduction-band offset of MoO_3 to the Si substrate, the energy levels of some traps introduced by the Mo doping in the LaMoO film should align with or lie above the valence band of the Si substrate. As a result, during the erasing process, injected holes from the Si substrate can directly recombine with the electrons trapped in the LaMoO film, and thus higher erasing speed can be achieved.[19]

Fig. 4 shows the charge retention characteristics of the two samples. To exclude the effect of internal electric field on charge loss, both samples are initially programmed to a similar memory window (3.98 V for the LaO sample under 14 V for 1 s, and 4.05 V for the LaMO sample under 12 V for 1 ms) before the charge-retention measurement. The deeper trap levels introduced by the Mo doping and the deeper quantum wells provided by the LaMoO CTL both induce better charge retention for the LaMO sample - 85.4% after 10 years, as compared to 77.6% of the LaO sample.

Conclusion

In this work, the memory characteristics of high-*K* La_2O_3 with and without Mo doping as charge-trapping layer were investigated. The memory device containing LaMoO film has much larger C-V hysteresis window, much higher P/E speeds, and better charge retention due to deeper-level traps generated by the Mo doing and deeper quantum wells created by the LaMoO film, both desirable for the purpose of charge trapping. Therefore, doping high-*K* dielectrics with suitable high-*K* NCBO material (e.g. MoO_3) is a promising method to improve the electrical performance of the high-*K* dielectrics used as the CTL of low-voltage memory devices.

Acknowledgement

This work is financially supported by the University Development Fund (Nanotechnology Research Institute, 00600009) of the University of Hong Kong.

References

1. G. H. Park, and W. J. Cho, *Appl. Phys. Lett.*, **96**, 043503 (2010).
2. T. M. Pan, W. W. Yeh, *J. Vac. Sci. Technol. A*, **27** (**4**), 700 (2009).
3. C. Mouli, K. Prall, and C. Roberts, *IPFA 14th International Symposium*, (2007), p.130.
4. T. M. Pan, and T. Y. Yu, *Semicond. Sci. Technol*. **24**, 095022 (2009).
5. H. J. Kim, S. Y. Cha, and D. J. Choi, *Materials Science in Semiconductor Processing*, **13**, 9 (2010).
6. G. D. Wilk, R. M. Wallace, and J. M. Anthony, *J. App. Phys.*, **89**, 5243 (2001).
7. B. Sen, H. Wong, J. Molina, H. Iwai, J. A. Ng, K. Kakushima, and C. K. Sarkar, *Solid-State Electronics*, **51**, 475 (2007).
8. C. C. Lin, and Y. Kuo, *ECS Journal of Solid State Science and Technology*, **2** (**1**), Q16 (2013).
9. X. Liu, C. H. Yang, Y. Kuo, and T. Yuan, *Electrochem. Solid-State Lett.*, **15** (**6**), H192 (2012).
10. B. D. Salvo, C. Gerardi, S. Lombardo, T. Baron, L. Perniola, D. Mariolle, P. Mur, A. Toffoli, M. Gely, M. N. Semeria, S. Deleonibus, G. Ammendola, V. Ancarani, M. Melanotte, R. Bez, L. Baldi, D. Corso, I. Crupi, R. A. Puglisi, G. Nicotra, E. Rimini, F. Mazen, G. Ghibaudo, G. Pananakakis, C. M. Compagnoni, D. Ielmini, A. Lacaita, A. Spinelli, Y. M. Wan, and K. V. Jeugd, *IEDM Tech. Dig.*, (2003), p. 597.
11. C. Y. Lu, T. C. Lu, and R. Liu, *IPFA 13th International Symposium*, (2006), p.18.
12. S. N. Keeney, *Proceedings-electrochemical society*, **4**, 151 (2004).
13. P. Mao, Z. Zhang, L. Pan, J. Xu, and P. Chen, *Appl. Phys. Lett.*, **93**, 242102 (2008).
14. D. B. Farmer, and R. G. Gordon, *J. Appl. Phys.*, **101**, 124503 (2007).
15. M. Sayer, A. Mansingh, J. B. Webb, and J. Noad, *J. Phys. C: Solid State Phys.*, **11**, 325 (1978).
16. Q. Y. Bao, J. P. Yang, Y. Q. Li, and J. X. Tang, *Appl. Phys. Lett.*, **97**, 063303 (2010).
17. M. T. Greiner, M. G. Helander, W. N. Tang, Z. B. Wang, J. Qiu, and Z. H. Lu, *nature materials*, **11**, 76 (2011).
18. D. Cao, X. H. Cheng, T.T. Jia. L. Zheng, D. W. Xu, Z. J. Wang, C. Xia, Y. H. Yu, and D. S. Shen, *IEEE Trans. On Nuclear Science*, in press.
19. X. G. Wang, J. Liu, W. P. Bai, and D. L. Kwong, *IEEE Trans. On Electron Devices*, **51,** 597 (2004)

Figure 1 (a) TEM image of the stacked gate dielectric structure of Al/Al_2O_3/LaMoO/SiO_2/Si after PDA treatment at 900 ^{0}C, (b) XPS of La 3*d* spectrum of the LaO sample and the LaMO sample, and (c) XPS of Mo 3*d* spectrum of the LaMO sample.

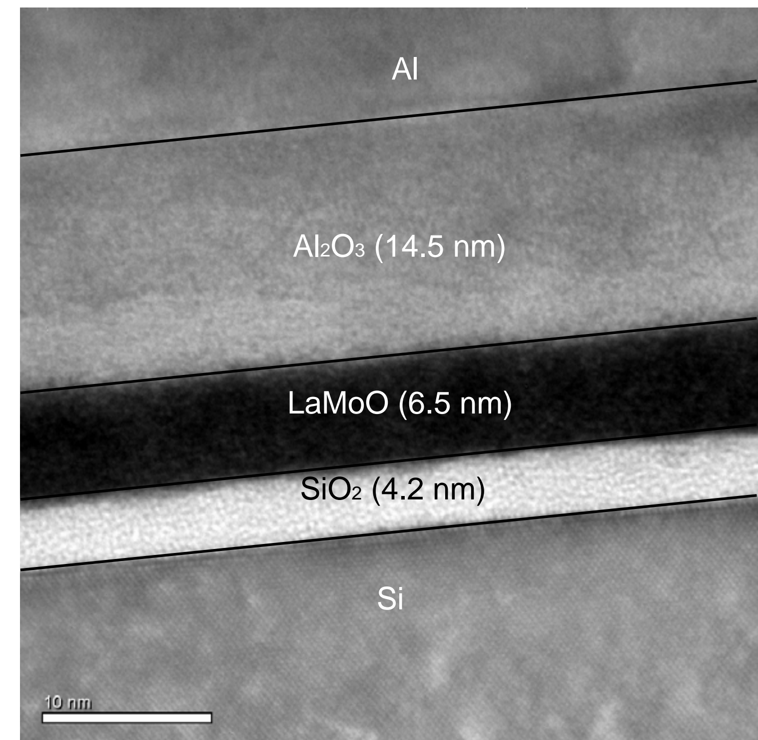

(a)

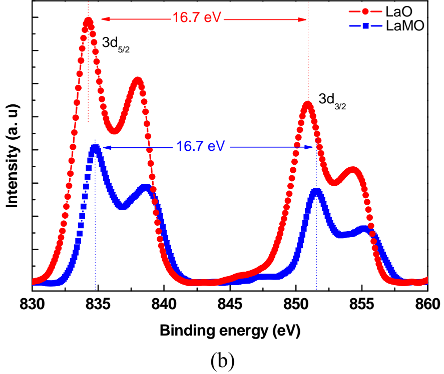

(b)

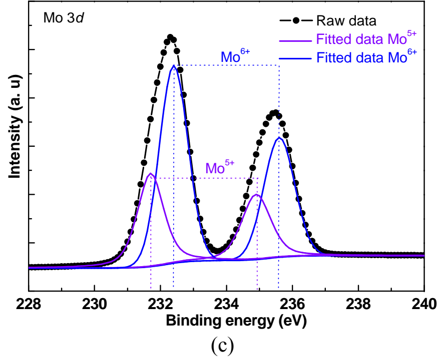

(c)

Figure 2 The C-V hysteresis properties of the LaO sample and the LaMO sample.

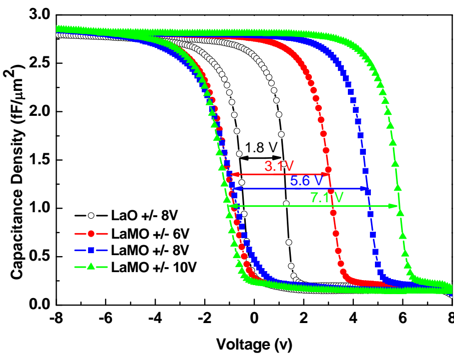

Figure 3(a) Program and (b) erase transient characteristics of the LaO sample and the LaMO sample.

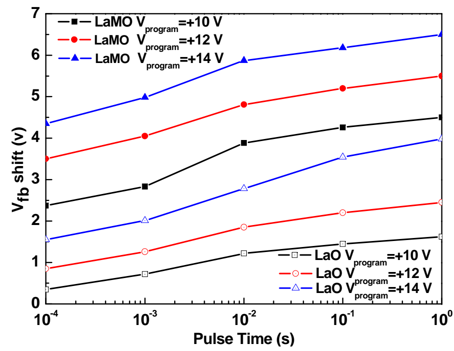

(a)

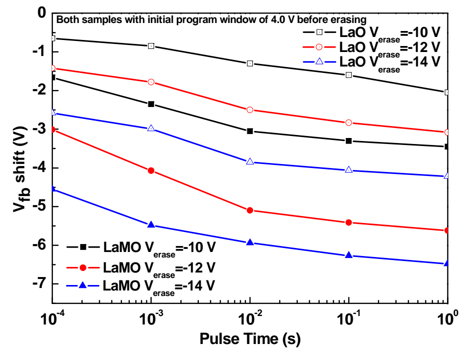

(b)

Figure 4 The charge retention characteristic of the LaO and LaMO samples.